Phase and surface area studies of maghemite nanoparticles dispersed in silica gel

Article *in* Materials Research Innovations · December 2014

DOI: 10.1179/1432891714Z.000000000927

3 authors, including:

Bee Chin Ang
University of Malaya
61 PUBLICATIONS **356** CITATIONS
SEE PROFILE

Yew Hoong Wong
University of Malaya
50 PUBLICATIONS **259** CITATIONS
SEE PROFILE

Phase and surface area studies of maghemite nanoparticles dispersed in silica gel

B. C. Ang*[1], I. I. Yaacob[2] and Y. H. Wong[1]

First, the superparamagnetic maghemite nanoparticles were synthesised using Massart's procedure. Then, the nanocomposites of the synthesised maghemite nanoparticles and silica were produced by dispersing the as-synthesised maghemite nanoparticles into the silica xerogel prepared by sol–gel technique. The system was then heated for 3 days at 140°C. The phase analysis performed using X-ray diffraction confirmed that the as-synthesised nanoparticles and the nanoparticles within the silica gel were maghemite. Surface characteristic of the nanocomposite was evaluated by N_2 adsorption. The 'pure' silica gel and maghemite nanoparticles showed high values of surface area (150–160 $m^2\,g^{-1}$), while the surface area of nanocomposite was less than 40 $m^2\,g^{-1}$. This was probably due to the formation of dense structures caused by incorporation of maghemite nanoparticles within the pores of silica gel. The pore width increased with increasing content of maghemite nanoparticles.

Keywords: Maghemite, Magnetic nanoparticles, Massart's procedure, Sol–gel, Nanocomposite

Introduction

Magnetic nanoparticles, with size ranging from 2 to 10 nm, are of particular importance because these particles are superparamagnetic and have very high surface areas. They are attracted to magnetic field gradient but retain no residual magnetism after the field is removed. They also show higher reactivity because they have enormously high values of surface area per volume. These particles can also be used in a number of practical applications such as medicine, ferrofluids, magnetic refrigeration systems and magnetic resonance imaging enhancement fluid.[1,2] However, these particles tend to aggregate and agglomerate to reduce the energy associated with their high surface area to volume ratio. Most of the unique properties are only present in properly dispersed particles and are no longer retained when they form agglomeration.

Several techniques are employed to control the agglomeration problem, such as coating the nanoparticles with surfactant and co-surfactant[3] and encapsulating the particles into silica gel using water in oil microemulsion technique.[1] Some researchers use one-step sol–gel method[4,5] to create a physical blockage to prevent interactions between the iron oxide nanoparticles and encapsulating it by using chitosan.[6] However, because of the instability in kinetic energy of the system, this method suffers from a major disadvantage. It is difficult to control the size and shape of the nanoparticles.

A two-step synthesis method was used in this study. In this technique, the maghemite nanoparticles were first synthesised using Massart's procedure.[3] This process produced nanoparticles in the desired size range, which was less than 10 nm. Second, the synthesised maghemite nanoparticles were encapsulated into silica gel matrix using sol–gel method.

These nanoparticles were incorporated within the nanopores of the silica gel matrix. The nanopores provided physical barriers in reducing the interaction between the nanoparticles and hence preventing them from aggregation or agglomeration. This method enabled us to obtain homogeneous and well-dispersed particles within silica matrix.

Experimental

The chemical reagents used were ferrous chloride hexahydrate (SIGMA), ammonium hydroxide (Fisher Chemical), ferric chloride (Fisher Chemical), ferric nitrate (AJAX), hydrochloric acid (AJAX) and nitric acid (Merck). The deionised water with resistivity of ~16–18 $M\Omega\,cm^{-1}$ was obtained using an ELGA ultra-analytic deioniser. All the reagents were of analytical grade and were used without any further purification.

Maghemite nanoparticles were synthesised by chemical coprecipitation as reported.[3] Powder specimen were obtained by drying the suspension in an oven at room temperature and labelled as M1. Dried Fe_2O_3 was used to proceed to the next step because Fe_2O_3 only stable in suspension with the pH level around 2·5. This pH level

[1]Center of Advanced Materials, Department of Mechanical Engineering, Faculty of Engineering, University of Malaya, Lembah Pantai, Kuala Lumpur 50603, Malaysia
[2]Department of Manufacturing and Materials Engineering, Kulliyyah of Engineering, International Islamic University Malaysia, P.O. Box 10, Kuala Lumpur 50728, Malaysia

*Corresponding author, email amelynang@um.edu.my

DOI 10.1179/1432891714Z.000000000927

will affect the formation of the silica gel and also the encapsulation process.

Nanocomposites consisting of as-synthesised maghemite nanoparticles and SiO_2 were prepared using sol–gel procedure. A typical sol–gel precursor mixture consisting of TEOS, tetrapropylammonium hydroxide solution and deionised water was used. The weight ratio of the precursor was 5:7:3, respectively. This sol–gel mixture was stirred overnight. The maghemite nanoparticles were then dispersed in the aged sol–gel mixture by stirring for additional 3 hours. This was followed by heating the system for a period of 3 days at 140°C. A number of samples with various weight ratios of Fe_2O_3/SiO_2 were prepared. The weight ratios of Fe_2O_3/SiO_2 investigated were 0·35, 0·7 and 1·4 and labelled as TF1, TF2 and TF3, respectively. A control sample of SiO_2 was prepared (without the addition of maghemite nanoparticles) and labelled as S1.

Characterisation

The structure and phase of the nanoparticles were examined by X-ray diffraction (XRD) using CuK_α radiation (Philips X-Pert MPD PW 3040). The XRD patterns were taken from 20° to 80° (2θ value). The mean crystallite size was deduced from the full-width at the half-maximum of three main peaks of the XRD pattern using Scherrer's relation.

N_2-physisorption measurements were collected on a Sorptomatic 1990 system (Thermo Finnigan). Before the analysis was carried out, all samples were outgassed at 120°C for 8 hours. The specific surface area (S_{BET}) and the total pore volume (V_p) were estimated by BET method.[7,8] The average pore width (d_p) was calculated from specific surface area and total pore volume.[9]

Transmission electron microscope (TEM) micrographs were recorded on a Leo LIBRA microscope, operated at 120 kV. The samples were taken from the N_2-physisorption measurements. They were ground into powders using agate mortar and dispersed in deionised water. Further, the dispersion process was done using an ultrasonic bath. A drop of the suspension was placed onto a conventional carbon-coated copper grid for observations. The average physical size was calculated by counting roughly 100 particles.

Results and discussion

Figure 1 shows the XRD patterns of M1, S1, TF1, TF2 and TF3 samples. All peaks in M1 sample match well with JCPDS card no. 39-1346. The calculated lattice parameter is 8·32 Å, which indicates that the sample is more likely to be maghemite (lattice parameter 8·33 Å) than magnetite (lattice parameter 8·396 Å).[10] The XRD pattern of S1 shows a broad diffraction shoulder at 2θ angle between 20° and 35° that corresponds to the pattern of amorphous silica gel.[11,12]

For samples of TF1, TF2 and TF3, the diffraction patterns show a broad shoulder of the silica gel and crystalline peaks, which originated from the maghemite nanoparticles. The patterns show the presence of only maghemite and SiO_2. This indicates that there is no chemical reaction between the silica gel and the maghemite nanoparticles to form other compounds. The broadening of (311), (511) and (440) reflections increases in the order of TF3, TF2 and TF1. The observed trend suggests that the crystallite size increases when the amount of maghemite nanoparticles in the silica matrix is increased. The average crystallite size of the samples calculated from the three major peaks by Scherrer's equation are 6, 5, 5 and 3 nm for samples M1, TF3, TF2 and TF1, respectively.

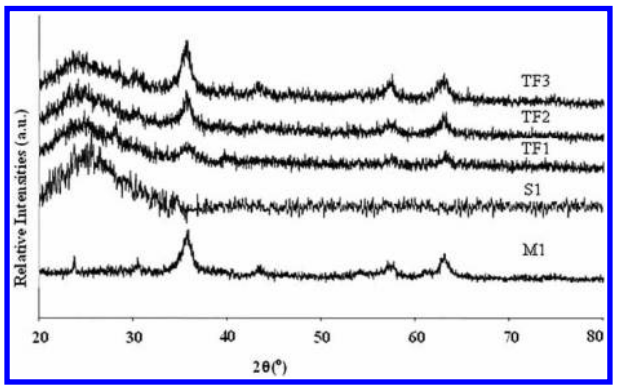

1 X-ray diffraction patterns for M1, S1, TF1, TF2 and TF3 samples

The average crystallite size of M1 is larger than the average crystallite size of TF samples, which indicates a slight dissolution of maghemite nanoparticles into silica gel.

Figure 2 shows a typical mesoporous graph for samples S1 and M1 with bigger hysteresis loop as compared to the TF samples (Fig. 3). The unique features are: (i) the adsorption at $P/P_o \rightarrow 0$ is moderately high compared to the TF samples, which indicates small amount of micropores; (ii) relative moderate increase of the adsorbed amount of N_2 in the P/P_o range of 0·1–0·9; (iii) a sharp increase of adsorbed N_2 in the P/P_o range of 0·9–1·0; (iv) the hysteresis loop is rather big and horizontally oriented; (v) the isotherms do not exhibit plateau at $P/P_o \rightarrow 1{\cdot}0$ but asymptotically approach to y-axis. All these features correspond relatively well to Type-IV isotherm.

A comparison is made on S1, M1 and TF1 samples. Among them, only the silica gel sample shows microporous behaviour. Larger hysteresis loop is observed for S1, because it contains higher number of pores.[7]

The features of isotherm changes as maghemite nanoparticles are added. The features are: (i) the adsorption

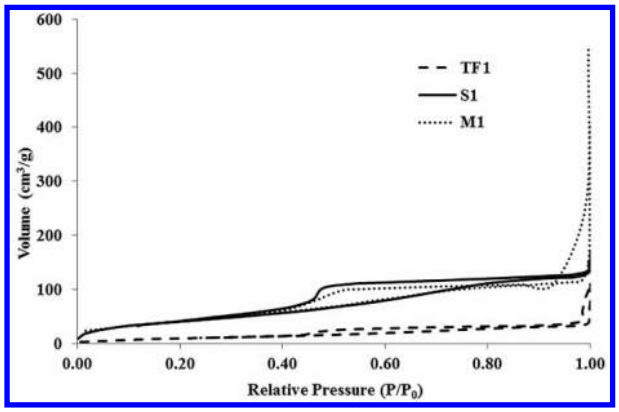

2 N_2-gas adsorption–desorption isotherms for M1, S1 and TF1 samples

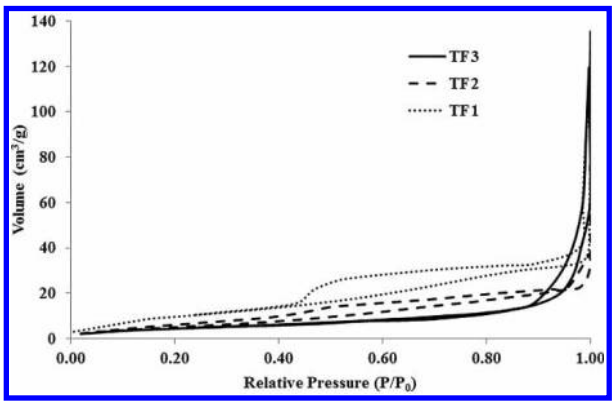

3 N_2-gas absorption–desorption isotherms for samples TF1, TF2 and TF3

at $P/P_o \rightarrow 0$ is very low, which indicates a very small amount of micropores for all TF's samples; (ii) relatively low increase of the adsorbed N_2 in the P/P_o range of 0·1–0·9; (iii) a sharp increase of the adsorbed N_2 in the P/P_o range from 0·9 to 1·0; (iv) the hysteresis loop is rather narrow and horizontally oriented; (v) the isotherms do not exhibit plateau at $P/P_o \rightarrow 1{\cdot}0$, but they asymptotically approach y-axis. All these features correspond relatively well to Type IVB isotherm, as shown in Fig. 3.

Smaller hysteresis loop is obtained when more maghemite nanoparticles are added. This indicates that the existing pores of silica gel are filled with the maghemite nanoparticles. The opening of the hysteresis loop for TF1 and TF2 samples at relatively lower pressure as compared to TF3 sample indicates that the distribution of the mesopores for TF1 and TF2 are shifted to lower pore diameter, d_p. This shows that most of the micropores of silica gel are filled when the amount of maghemite nanoparticles reached a certain value. This is illustrated by the typical pore size distribution calculated by How/Kar method, as shown in Fig. 4 and Table 1.

The surface area obtained for nanocomposite samples (TF) is much lower compared to sample of silica (S1) and maghemite nanoparticles (M1). By increasing the content of maghemite nanoparticles, the surface area of the nanocomposite system reduces. This suggests that the pores of silica matrix are almost fully filled. From the TEM image (Fig. 4), it is clear that the embedded maghemite nanoparticles are isolated. The calculated crystallite and physical sizes from XRD and TEM prove that the sizes of embedded nanoparticles are smaller than original maghemite nanoparticles.[13,14]

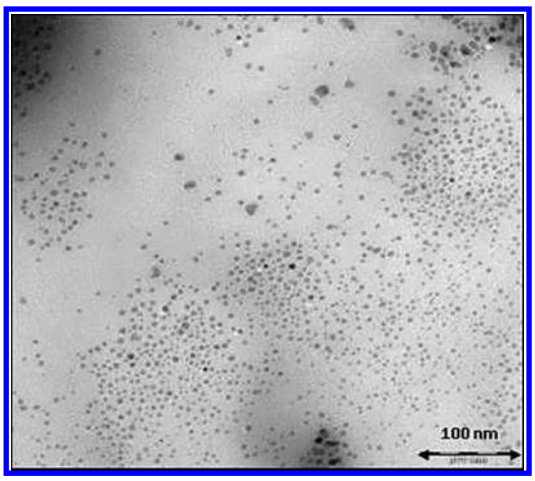

4 Transmission electron microscope image of TF1

Table 1 Parameters calculated from N_2 adsorption isotherms

Sample	S_{BET} (BET) ($m^2\ g^{-1}$)	V_p (BET) ($cm^3\ g^{-1}$)	d_p ($4V_p/S_p$) (nm)
M1	156	0·23	6·0
S1	155	0·19	4·9
TF1	38	0·05	4·9
TF2	21	0·07	13·9
TF3	17	0·06	14·4

Conclusion

This study showed that maghemite–silica gel nanocomposites were formed successfully. The N_2-gas adsorption–desorption hysteresis loops of maghemite–silica samples became smaller with increasing content of maghemite nanoparticles within silica matrix. This indicated that the amount of pores has reduced. This was further proved by observing the average pore width. The hysteresis loops showed that macro- and micropores of SiO_2 are filled. The crystallite size of the embedded particles was smaller than the as-synthesised nanoparticles, indicating that a slight dissolution of particles occurred during encapsulation process.

Acknowledgment

This research is supported by University Malaya Research Grant (RP021-2012C) under Institute of Research, University of Malaya.

References

1. H. H. Yang, S. Q. Zhang, X. L. Chen, Z. X. Zhuang, J. G. Xu and X. R. Wang: 'Magnetite-containing spherical silica nanoparticles for biocatalysis and bioseparations', *Anal. Chem.*, 2004, **76**, 1316–1321.
2. M. Aslam, L. Fu, S. Li and P. D. Vinayak: 'Silica encapsulation and magnetic properties of FePt nanoparticles', *J. Colloid Interface Sci.*, 2005, **290**, (2), 444–449.
3. B. C. Ang and I. I. Yaacob: 'Synthesis and characterization of magnetic iron oxide nanoparticles via w/o microemulsion and Massart's procedure', *J. Mater. Process. Technol.*, 2007, **191**, (1–3), 235–237.
4. C. Cannas, M. Casu, A. Musinu and G. Piccaluga: 'Si CPMAS NMR and near-IR study of sol-gel microporous silica with tunable surface area', *J. Non-Cryst. Solids*, 2005, **351**, 3476–3482.
5. P. M. Zelis, M. B. F. Van Raap, L. M. Socoloysky, A. G. Leyya and F. H. Sanchez: 'Magnetic hydrophobic nanocomposites: silica aerogel/maghemite', *Physica B – Condensed Matter*, 2012, **407**, (16), 3113–3116.
6. R. Jiang, Y. Q. Fu, H. Y. Zhu, J. Yao and L. Xiao: 'Removal of methyl orange from aqueous solutions by magnetic maghemite/chitosan nanocomposite films: Adsorption kinetics and equilibrium', *J. Appl. Polym. Sci.*, 2012, **125**, E540–E549.
7. S. J. Gregg and K. S. W. Sing: '*Adsorption, Surface Area and Porosity*', 2nd edn; 1982, London, Academic Press.
8. S. Brunauer, P. H. Emmett and E. Teller: 'Adsorption of gases in multimolecular layers', *J. Am. Chem. Soc.*, 1938, **60**, 309–319.
9. M. S. K. Kamal and A. M. Salah: 'High surface area thermally stabilized porous iron oxide/silica nanocomposites via a formamide modified sol-gel process', *Appl. Surf. Sci.*, 2008, **254**, 3767–3773.
10. A. G. Roca, M. P. Morales, K. O. Grady and C. J. Serna: 'Structural and magnetic properties of uniform magnetite nanoparticles

prepared by high temperature decomposition of organic precursor', *J. Nanotechnol.*, 2006, **17**, 2783–2788.
11. J. P. Rainho, J. Rocha, L. D. Carlos and R. M. Almeida: 'Si nuclear-magnetic-resonance and vibrational spectroscopy studies of SiO_2–TiO_2 powders prepared by the sol–gel process', *J. Mater. Res.*, 2001, **16**, 2369.
12. E. Barrado, J. A. Rodriguez, F. Prieto and J. Medina: 'Characterization of iron oxides embedded in silica gel obtained by two different methods', *J. Non-Cryst. Solids*, 2005, **351**, 906–914.
13. B. C. Ang and I. I. Yaacob: 'Preparation of maghemite-silica nanocomposite using sol-gel technique', *Adv. Mater. Res.*, 2010, **97–101**, 2140–2143.
14. B. C. Ang, I. I. Yaacob and Irwan Nurdin: 'Investigation of Fe_2O_3/SiO_2 nanocomposite by FESEM and TEM', *J. Nanomater.*, 2013, **2013**, 980390.